Available online at www.sciencedirect.com
ScienceDirect
Trans. Nonferrous Met. Soc. China 20(2010) 1177−1183
Transactions of Nonferrous Metals Society of China
www.tnmsc.cn

Influence of $GdCl_3$ addition on purifying effectiveness and properties of Mg-10Gd-3Y-0.5Zr alloy

WU Guo-hua(吴国华)[1, 2], WANG Wei(王 玮)[1, 2], SUN Ming(孙 明)[1, 2],
WANG Qu-dong(王渠东)[1, 2], DING Wen-jiang(丁文江)[1, 2]

1. National Engineering Research Center of Light Alloy Net Forming, Shanghai Jiao Tong University, Shanghai 200240, China;
2. State Key Laboratory of Metal Matrix Composites, Shanghai Jiao Tong University, Shanghai 200240, China

Received 23 September 2009; accepted 30 January 2010

Abstract: In order to improve the purifying efficiency of RJ6 flux, 5% (mass fraction) $GdCl_3$ was introduced into the flux for refining Mg-10Gd-3Y-0.5Zr (GW103K) alloy. The results show that the RJ6 flux containing 5% $GdCl_3$ exhibits better adsorption ability to nonmetallic inclusions than the one without $GdCl_3$. Moreover, the mechanical, corrosion properties and fluidity of the alloy refined with RJ6 flux and RJ6 flux containing 5% $GdCl_3$ were investigated, respectively. It is found that these properties are improved to a certain degree due to the removal of nonmetallic inclusions in the alloy. Thermodynamic analysis and surface tension experiments indicate that the main reason can be ascribed to the decrease of the surface tension of the flux with 5% $GdCl_3$, which promotes the combination of flux and nonmetallic inclusions.
Key words: magnesium alloy; rare earth element; nonmetallic inclusions; refining; corrosion; fluidity

1 Introduction

Mg-10Gd-3Y-0.5Zr (GW103K) magnesium alloy has been widely investigated due to its prominent mechanical properties. This alloy shows great application prospect in automobile industry because of its higher specific strength at both room and elevated temperatures and better creep resistance than other Mg-rare earth (RE) alloys such as WE54[1−6]. However, magnesium and rare earth elements tend to oxidize rapidly during the course of smelting due to their high chemical activities. These oxide inclusions destroy the continuity of the magnesium matrix, induce the defects of pores and cracks, and then impair the mechanical, corrosion and fluidity properties of the alloys[7−8]. Therefore, removing these nonmetallic inclusions from the alloy becomes an urgent task currently.

Traditional flux refining process is always accepted as one of the most effective purifying methods because of its high purifying efficiency, low cost, and being easy to realize. $MgCl_2$ in flux has been widely considered as one of the main ingredients because liquid $MgCl_2$ has an excellent adsorption capability to MgO inclusions and forms $MgCl_2·5MgO$ compounds which could sink to the bottom of crucible. For GW103K alloy, however, the expensive heavy RE elements, Gd and Y, tend to react with $MgCl_2$ and then result in the burn loss during the course of refining. Therefore, the flux without $MgCl_2$, such as RJ6 flux, was engaged to purify RE containing magnesium alloys. But the purifying effects are not as good as the one containing $MgCl_2$[9]. Actually, the lack of efficient purification processes even becomes a bottleneck which limits the application of GW103K alloy.

In this work, in order to improve the purifying ability, 5% (mass fraction) $GdCl_3$ was introduced into RJ6 flux. The surface tensions of the fluxes used in the experiments were determined and its purification mechanism was explained by thermodynamic calculation. The mechanical, corrosion properties and fluidity of GW103K alloy refined with RJ6+5% (mass fraction) $GdCl_3$ additions were investigated as well.

2 Experimental

Pure $GdCl_3$ was added into RJ6 flux and mixed in

Foundation item: Project(08XD14020) supported by Program of Shanghai Subject Chief Scientist; Project(2007CB613701) supported by the National Basic Research Program of China; Project(2009AA033501) supported by High-tech Research and Development Program of China
Corresponding author: WU Guo-hua; Tel: +86-21-54742630; Fax: +86-21-34202794; E-mail: ghwu@sjtu.edu.cn
DOI: 10.1016/S1003-6326(09)60275-2

QM-ISP pebble mill for 3 h. The composition of RJ6 flux containing 5% $GdCl_3$ is listed in Table 1.

Table 1 Composition of RJ6+5% $GdCl_3$ flux (mass fraction, %)

KCl	$BaCl_2$	CaF_2	$CaCl_2$	NaCl+$CaCl_2$	$GdCl_3$	Insolubles
54−56	14−16	1.5−2.5	27−29	8	5	1.5

GW103K alloy was fabricated by pure Mg ingots and Mg-Gd, Mg-Y, Mg-Zr master alloys. Smelting was performed in a 7 kW crucible electric resistance furnace under protection of a shield gas consisting of SF_6 (1%, volume fraction) and CO_2 (99%, volume fraction). 2.5% (mass ratio to the whole raw metal) new fluxes were added to refine the melt at 760℃. The melt was held for 30−45 min after refining, and then poured at 740 ℃ into the metallic molds which were preheated up to 400 ℃.

Tensile tests were conducted on a Zwick/Roell electronic universal material testing machine. For the specimens tested in T6 condition, the heat treatment method was: solution treatment at 500 ℃ for 8 h in argon atmosphere, and peak-ageing at 225 ℃ in an oil bath for 16 h. The Rigaku Dmax-rc X-ray diffractometer and PHILIPS SEM 515 were employed to analyze phase composition and corrosion morphology, respectively. The composition of inclusions was analyzed with energy dispersive spectroscope (EDS) attached to the SEM.

The size of specimens for immersion corrosion tests was d35 mm×4 mm. The specimens were polished successively on fine grades of emery papers up to 800 grit, and then immersed in a 5% (mass fraction) NaCl aqueous solution at room temperature ((25±0.5) ℃). After three days immersion, the specimens were cleaned by dipping in a solution of 15% Cr_2O_3+1% $AgNO_3$ in 500 mL water in boiling condition. The corrosion rates were obtained in mass loss per surface area and time ($mg{\cdot}cm^{-2}{\cdot}d^{-1}$).

Fluidity of the alloy was measured as the length of the metal flow in the spiral-shaped metallic mould (Fig.1). The Archimedian spiral has a cross section of 4 mm×10 mm with a maximum running length of 1.4 m. In order to analyze the influence of nonmetallic inclusions on the fluidity of GW103K alloy, the pouring temperature was the same as casting condition (740 ℃) and the mould preheating temperature was limited to 400 ℃ because higher mould temperatures would promote mould−metal reactivity and then cause a deleterious effect on surface finish.

Statistical volume fractions of nonmetallic inclusions in the alloy were measured with Leco image software. The purifying abilities of the fluxes were determined by comparing the volume fractions of nonmetallic inclusions before and after refining.

The surface tensions of the fluxes were determined

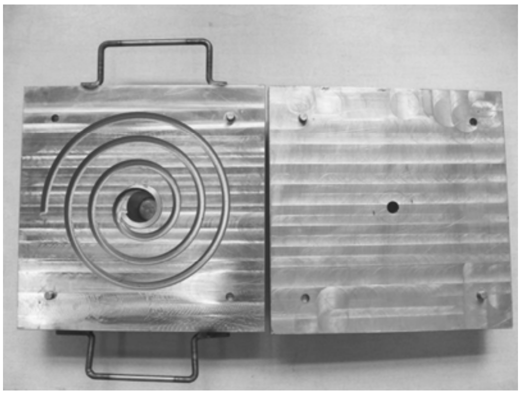

Fig.1 Open mould showing spiral-shaped permanent mould

by RTW-05 Flux Properties Admeasuring Apparatus at 760 ℃ (refining temperature).

3 Results and discussion

3.1 Purifying effectiveness

Before analyzing the purifying effectiveness, it is necessary to clarify the main ingredients and morphologies of nonmetallic inclusions in the alloy. Previous work[10−11] showed that the largest inclusions in GW103K alloy exhibited spherical, bar-shape and irregular morphology. In addition, some fine inclusions were dispersed within grains and on the grain boundary. The composition of these nonmetallic inclusions was determined by EDS analysis as shown in Fig.2. The result indicates that these nonmetallic inclusions are mainly MgO, chlorides and oxides of Gd and Y.

The purifying effectiveness of the two fluxes was examined by comparing the contents of nonmetallic inclusions in the alloy before and after refining. Table 2 shows the statistical volume fractions of nonmetallic inclusions in the alloy. It is clear that the specimen refined by RJ6+5% $GdCl_3$ addition exhibited the lowest average volume fraction (1.03%). This indicates that the purifying effectiveness of RJ6+5% $GdCl_3$ addition is better than that of pure RJ6 flux.

Generally, the course of removing nonmetallic inclusions from melts by flux can be divided into the following three steps: first, the collision occurs between nonmetallic inclusions and molten flux; next, the flux adsorbs nonmetallic inclusions; finally, the inclusion drops together with flux down to the bottom of the crucible. Here, the second step is widely regarded as the restrictive link of the three. The change of Gibbs free energy of this step could be expressed as

$$-\Delta G=[\sigma_{\mathrm{m-i}}-(\sigma_{\mathrm{f-i}}+\sigma_{\mathrm{m-f}})]\Delta\omega \quad (1)$$

where $\sigma_{\mathrm{m-i}}$, $\sigma_{\mathrm{f-i}}$ and $\sigma_{\mathrm{m-f}}$ are interface tensions among melt, inclusion and flux; and $\Delta\omega$ is the increment of

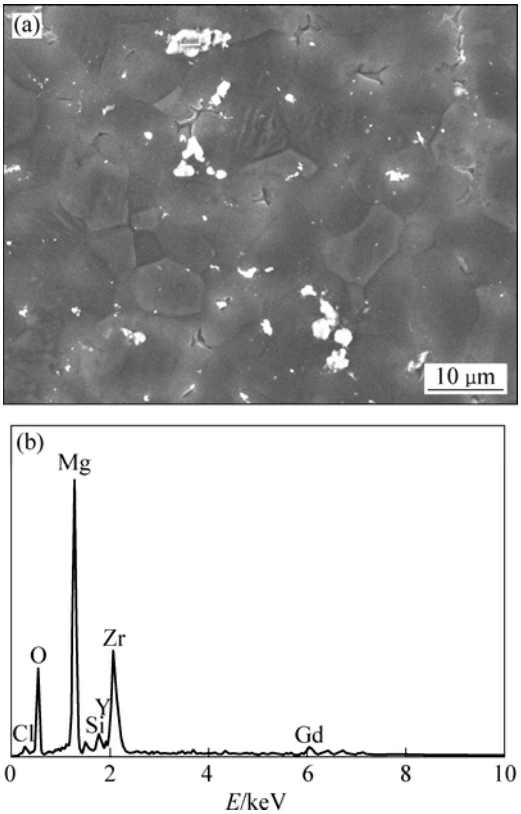

Fig.2 SEM image and EDS pattern of inclusion in GW103K alloy

Table 2 Statistical volume fraction of inclusions in GW103K alloys with different treatments

Refining flux	Number of fields	Average volume fraction/%
Unrefined	30	4.07
Pure RJ6	30	2.84
RJ6+5% $GdCl_3$	30	1.03

surface area.

As can be seen from Eq.(1), ΔG will be more negative with the decrease of σ_{m-f} and σ_{f-i} while σ_{m-i} is unchanged. The decrease of σ_{m-f} makes it easy for nonmetallic inclusions to transfer from magnesium melts to the flux. Once the inclusions move to the surface of the molten flux, the low σ_{f-i} would make them captured by flux easily. As shown in Table 3, the surface tension of RJ6+5% $GdCl_3$ flux is 0.161 N/m at 760 ℃, which is lower than pure RJ6 flux (0.212 N/m). Inevitably, the interface tension σ_{f-i} decreases with the decrease of the surface tension of the flux and then promotes the combination of flux and nonmetallic inclusion. Therefore, the RJ6+5% $GdCl_3$ flux exhibit better purifying ability than pure RJ6 flux.

Table 3 Surface tension (at 760 ℃) of fluxes used in experiments (N/m)

RJ6	RJ6+5% $GdCl_3$
0.212	0.161

3.2 Microstructure

Fig.3 shows the microstructures of GW103K alloy (as-cast) refined with RJ6+5% $GdCl_3$ and pure RJ6 flux, respectively.

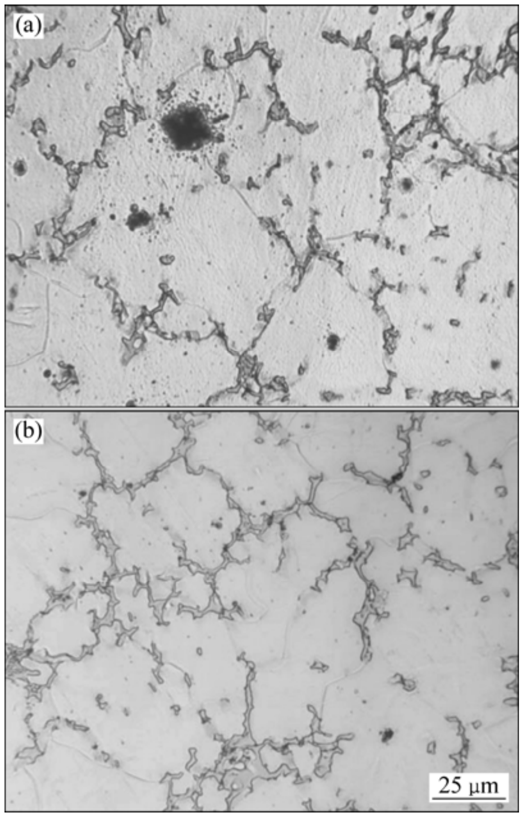

Fig.3 Microstructures of GW103K alloy (as-cast) with different purifying fluxes: (a) RJ6; (b) RJ6+5% $GdCl_3$

For the specimens refined with RJ6+5%$GdCl_3$ flux, it can be seen that the fraction of the inclusions is lower than that in specimens refined by pure RJ6 flux. The compositions of phases of GW103K alloy unrefined (Fig.4(a)) and refined with RJ6+5% $GdCl_3$ (Fig.4(b)) were identified using XRD. The results indicate that the phase compositions of the alloy have not been changed. They all still consist of matrix α-Mg and second phase Mg-Gd-Y compounds. It could be concluded that the refining treatments almost have no influence on the microstructures of GW103K alloy.

In T6 condition, the microstructures are different from as-cast condition, as shown in Fig.5. All of the eutectic phases dissolve into the matrix only with some inclusions and quadrate precipitates remained.

The fracture surfaces of the specimens in as-cast condition after tensile tests are shown in Fig.6. It is clear that the fracture pattern has not been changed after the refining process. The fracture mechanisms are still

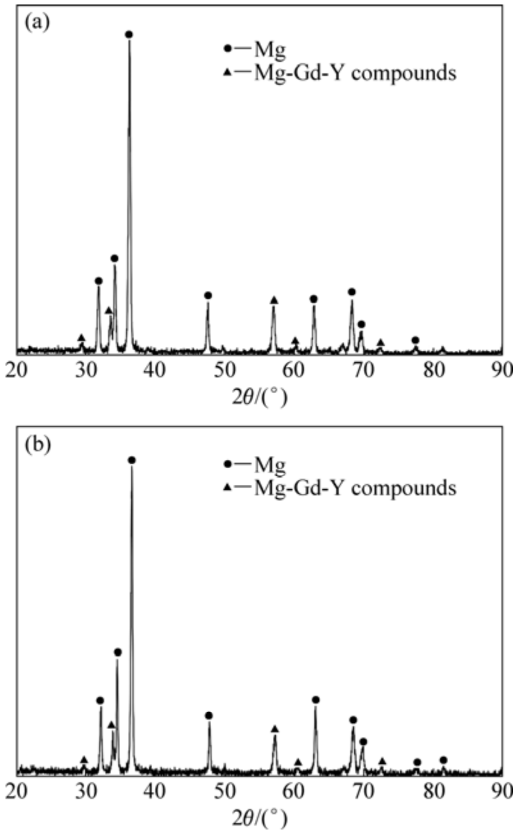

Fig.4 XRD patterns of GW103K alloy under different treatment conditions: (a) Unrefined: (b) Refined by RJ6+5% $GdCl_3$

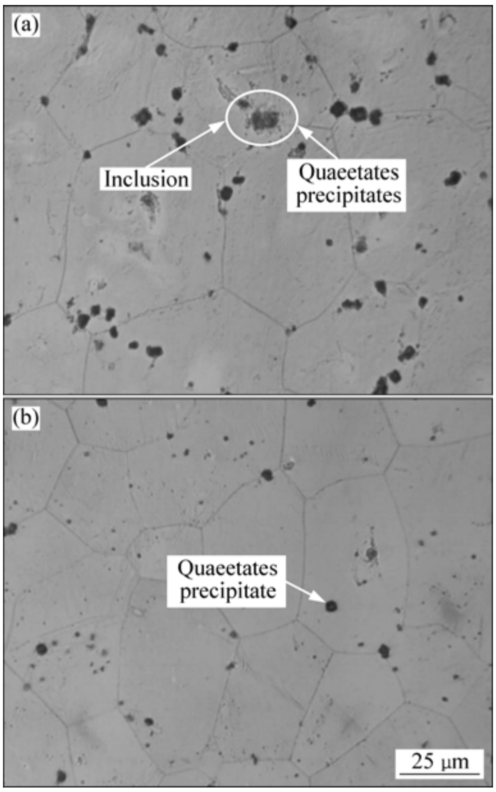

Fig.5 Microstructures of GW103K alloy (T6 conditions) under different treatment conditions: (a) Unrefined; (b) Refined with RJ6+5% $GdCl_3$

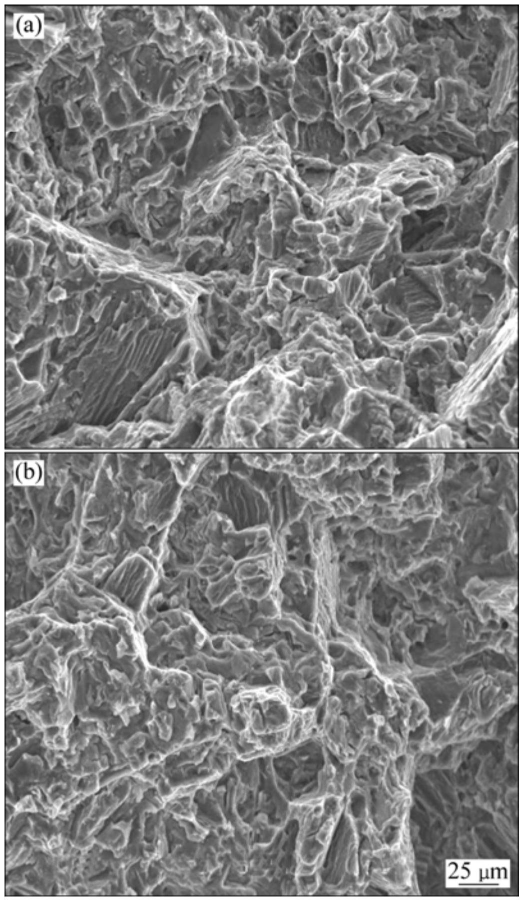

Fig.6 Fractographs of tensile samples of GW103K alloy under as-cast condition: (a) Unrefined; (b) Refined by RJ6+5% $GdCl_3$

quasi-cleavage crack.

3.3 Mechanical properties

Fig.7 shows the effects of different purification treatments on mechanical properties of GW103K alloy.

In as-cast condition, the relationship between the mechanical properties and different refining methods is shown in Fig.7(a). Compared with the specimens refined with pure RJ6 flux, the ultimate tensile strength (σ_b), yield strength at 0.2% offset (σ_s) and elongation (δ) of the specimens refined with RJ6+5%$GdCl_3$ were improved from 197.46 MPa, 157.67 MPa and 0.69% to 213.86 MPa, 179.66 MPa and 0.82%, respectively. Meanwhile, for the unrefined specimens, σ_b, σ_s and δ are only 182.25 MPa, 136.47 MPa and 0.51%, respectively. In T6 condition (Fig.7(b)), the mechanical properties are similar to those in the as-cast condition. The best combination of tensile properties (σ_b, σ_s and δ) is still achieved with the 5% $GdCl_3$ additions. σ_b, σ_s and δ reach 310 MPa, 244.1 MPa and 0.76%, respectively.

In general, whether under as-cast or T6 condition, the best combination of mechanical properties of GW103K alloy could be obtained when being refined with RJ6+5% $GdCl_3$ flux, especially for elongation. As

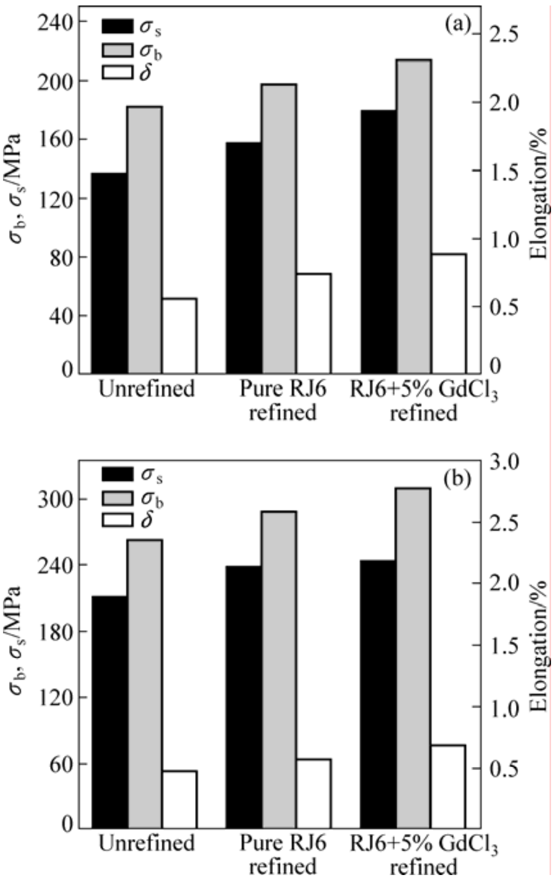

Fig.7 Mechanical properties of GW103K alloy under different treatment conditions: (a) As-cast; (b) T6 condition

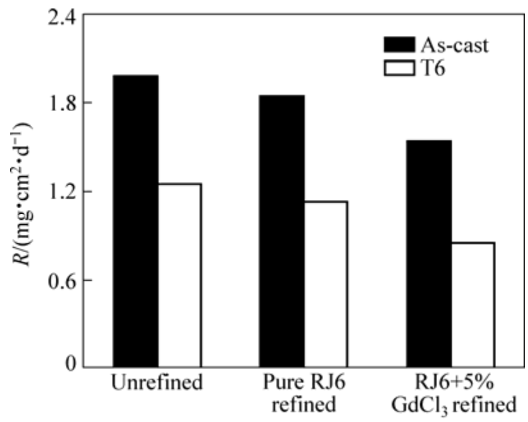

Fig.8 Corrosion rates of GW103K alloy under different treatment conditions

stated before, the nonmetallic inclusions in alloy cut off the continuity of the matrix, cause stress constrain, supply flaw recourses and thus impair the mechanical properties. Hence, the improvement of the mechanical properties could be ascribed to the excellent ability of removing nonmetallic inclusions by RJ6+5% $GdCl_3$ flux.

3.4 Corrosion resistance

The corrosion rates of GW103K alloy treated with different refining processes are shown in Fig.8. Whether in as-cast or T6 condition, the specimen refined with RJ6+5% $GdCl_3$ exhibits the lowest corrosion rate. The corrosion resistance is enhanced in the following sequence: unrefined<pure RJ6<RJ6+5%$GdCl_3$. In as-cast condition, compared with specimens refined with pure RJ6 flux, the corrosion rate of the specimens refined with RJ6+5%$GdCl_3$ decreases from 1.84 to 1.54 mg/(cm^2·d).

Fig.9 shows the morphological characteristics of the corroded surfaces of the specimens immersed in 5% NaCl aqueous solution for 3 d. It can be seen that deep corrosion pits distribute on the surface of the specimens except the one refined with RJ6+5% $GdCl_3$. Maybe it could be deduced that corrosion develops from the nonmetallic inclusions on the surface of the alloy.

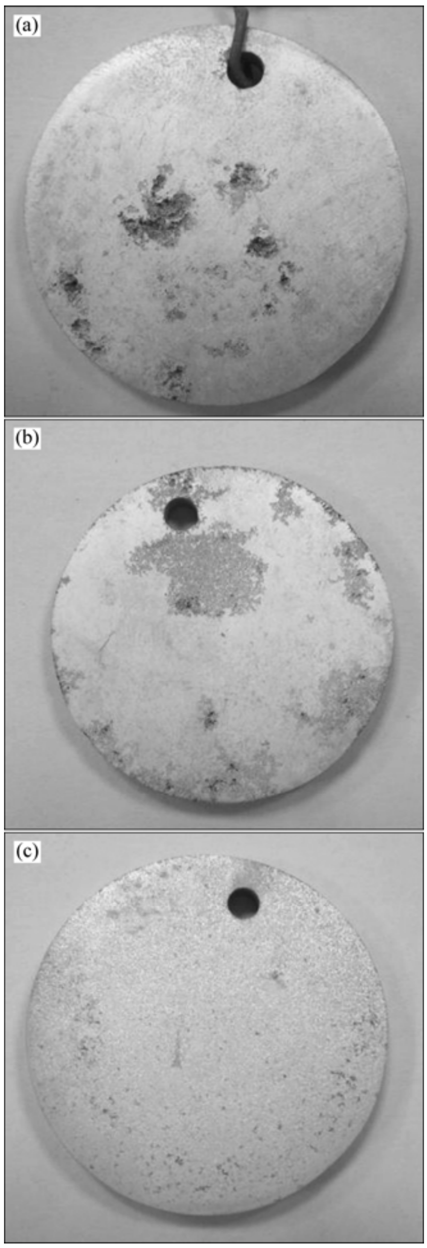

Fig.9 Surface corrosion morphologies of GW103K alloy after being immersed in 5% NaCl aqueous solution for 3 d: (a) Unrefined; (b) Pure RJ6 refined; (c) RJ6+5% $GdCl_3$ refined

For the specimens in T6 condition, the corrosion rates are generally lower than those in as-cast condition (Fig.8). This could be ascribed to the change of phase compositions in alloy. It could be found from Fig.3 and Fig.5 that the network eutectic phases in as-cast condition have dissolved into the α-Mg matrix after T6 heat treatment, only some quadrate precipitates and nonmetallic inclusions remained. It was reported[12] that the eutectic phase acted as cathode and formed galvanic coupling corrosion with the Mg matrix when corrosion happened, and then speeded up the corrosion process. Therefore, with the decrease of the fraction of eutectic phase, the alloy in T6 condition exhibits better corrosion resistance than that in as-cast condition.

Whether in as-cast or T6 condition, the galvanic coupling, which accelerates the corrosion rates[13], could be formed between the nonmetallic inclusions and magnesium matrix during the course of corrosion. As shown in Table 2, the RJ6+5% $GdCl_3$ additions exhibit remarkable ability of removing nonmetallic inclusions. The reduction of nonmetallic inclusions decreases the cathode areas and thus improves the corrosion resistance of the alloy.

3.5 Fluidity

It is clear from Fig.10 that GW103K alloy melt refined with RJ6+5% $GdCl_3$ has a much larger fluidity length (1 113 mm) than that of unrefined (780 mm) and refined with pure RJ6 flux (828 mm). Combined with the results in Table 2, we can infer that the fluidity lengths will increase when the volume fractions of nonmetallic inclusions decrease.

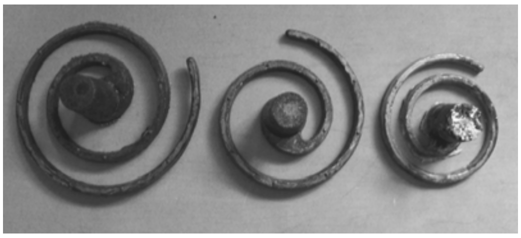

Fig.10 Fluidity of GW103K alloy with different treatments: (a) RJ6+5% $GdCl_3$ refined; (b) Pure RJ6 refined; (c) Unrefined

RAVI et al[14] reported that the viscosity of the melt was an important parameter which influences the fluidity greatly. SURAPPA and ROHATGI[15] observed that the increase in the viscosity of the melt due to dispersions of nonmetallic inclusions appeared to be one of the major reasons for the decrease in spiral fluidity of the alloy. For dilute suspensions (solid volume fraction, $\varphi < 0.25$), the viscosity of the suspension can be estimated using Einstein's equation:

$$\mu_c = \mu_0[1 + 2.5\varphi + 10.25\varphi^2] \tag{2}$$

where μ_c is the apparent viscosity, μ_0 is the viscosity of fluids without any particle and φ is the volume fraction of nonmetallic inclusions in the alloy melt. Eq.(2) suggests that the apparent viscosity rises markedly compared with the viscosity of pure melts when the volume fraction of nonmetallic inclusions increases. It could be concluded that the viscosity of the alloy melt would decrease after being refined with RJ6+5% $GdCl_3$ because of its high purifying efficiency. Therefore, the melt refined with RJ6+5% $GdCl_3$ exhibits excellent fluidity.

4 Conclusions

1) The addition of 5% $GdCl_3$ into RJ6 flux decreases the surface tension of the flux, which improves the purification effectiveness of the flux.

2) The mechanical properties of GW103K alloy both in as-cast and T6 conditions are greatly enhanced by RJ6+5% $GdCl_3$ addition. The ultimate tensile strength, yield strength at 0.2% offset and elongation reach the maximum values of 213.86 MPa, 179.66 MPa and 0.82% for as-cast condition, and 310 MPa, 244.1 MPa and 0.76% for T6 condition.

3) The corrosion rate of the alloy refined by RJ6+5%$GdCl_3$ flux declines to the minimum of 1.54 mg/(cm^2·d) for as-cast specimens.

4) The fluidity of GW103K alloy melt refined with RJ6+5% $GdCl_3$ is greatly improved due to the decrease of viscosity.

Acknowledgements

The authors would like to thank the Center of Analysis and Measurement of Shanghai Jiao Tong University for assistance with the XRD and the field emission scanning electron microscope (FE-SEM).

References

[1] HE S M, ZENG X Q, PENG L M, GAO X, NIE J F, DING W J. Microstructure and strengthening mechanism of high strength Mg-10Gd-2Y-0.5Zr alloy [J]. Journal of Alloys and Compounds, 2007, 427(1): 316−323.

[2] HE S M, ZENG X Q, PENG L M, GAO X, NIE J F, DING W J. Precipitation in a Mg-10Gd-3Y-0.4Zr (wt.%) alloy during isothermal aging at 250 ℃ [J]. Journal of Alloys and Compounds, 2006, 421(1/2): 309−313.

[3] SMOLA B, STULIKOVA F, von BUCH F, MORDIKE B L. Structural aspects of high performance Mg alloys design [J]. Materials Science and Engineering A, 2002, 324(1/2): 113−117.

[4] SUN Y C, CONG F G, GUAN F L, SUN X M. Refing study for magnesium alloy scrap [J]. Light Alloy Fabrication Technology, 2006, 34(2): 11−20. (in Chinese)

[5] ANYANWU I A, KAMADO S, KOJIMA Y. Aging characteristics and high temperature tensile properties of Mg-Gd-Y-Zr alloys [J]. Materials Transaction, 2001, 42(7): 1206−1211.

[6] ANYANWU I A, KAMADO S, KOJIMA Y. Creep properties of Mg-Gd-Y-Zr alloys [J]. Materials Transaction, 2001, 42(7): 1212−1218.

[7] DU W B, WU Y F, NIE Z R, SU X K, ZUO T Y. Effects of rare earth and alkaline earth on magnesium alloys and their applications status [J]. Rare Metal Materials and Engineering, 2006, 35(9): 1345−1348. (in Chinese)

[8] GAO H T, WU G H, DING W J, ZHU Y P. Study on Fe reduction in AZ91 melt by B_2O_3 [J]. Materials Science and Engineering A, 2004, 368(1/2): 530−536.

[9] CHENG Z H. Magnesium alloy [M]. Beijing: Chemical Industry Press, 2004. (in Chinese)

[10] WANG W, WU G H, WANG Q D, HUANG Y G, DING W J. Gd contents, mechanical and corrosion properties of Mg-10Gd-3Y-0.5Zr alloy purified by fluxes containing $GdCl_3$ additions [J] Materials Science and Engineering A, 2009, 507: 207−214.

[11] WANG W, HUANG Y G, WU G H, WANG Q D, SUN M, DING W J. Influence of flux containing YCl_3 additions on purifying effectiveness and properties of Mg-10Gd-3Y-0.5Zr alloy [J]. Journal of Alloys and Compounds, 2009, 480: 386−391.

[12] GUO X W, CHANG J W, HE S M, DING W J. Investigation of corrosion behaviors of Mg-6Gd-3Y-0.4Zr alloy in NaCl aqueous solutions [J]. Electrochimica Acta, 2007, 52(7): 2570−2579.

[13] GAO H T, WU G H, FAN Y, DING W J, ZHU Y P. Effect of $CeCl_3$ on loss of Ce in magnesium alloy during refining [J]. The Chinese Journal of Nonferrous Metals, 2005, 15(12): 2003−2008. (in Chinese)

[14] RAVI K R, PILLAI R M, AMARANATHAN K R, PAI B C, CHAKRABORTY M. Fluidity of aluminum alloys and composites: A review [J]. Journal of Alloys and Compound, 2008, 456(1/2): 201−210.

[15] SURAPPA M K, ROHATGI P K. Fluidity of aluminum-silicon-alumina composite [J]. Metallurgical Transactions B, 1981, 12(2): 327−332.

(Edited by YANG Bing)